Experimental characterisation and modelling of the thermo-viscoplastic behaviour of steel AISI 304 within wide ranges of strain rate at room temperature

Alexis Rusinek, José A. Rodriguez-Martinez, Raphaël Pesci, Julien Capelle

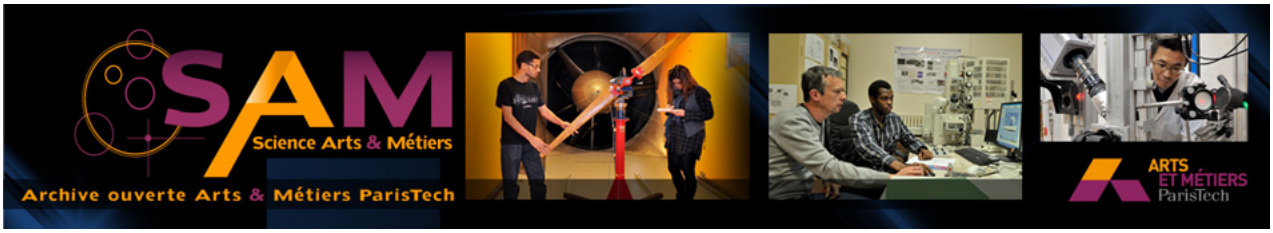

EXPERIMENTAL CHARACTERISATION AND MODELLING OF THE THERMO-VISCOPLASTIC BEHAVIOUR OF STEEL AISI 304 WITHIN WIDE RANGES OF STRAIN RATE AT ROOM TEMPERATURE

Alexis Rusinek
National Engineering School of Metz (ENIM), Laboratory of Mechanics, Biomechanics, Polymers and Structures, Metz cedex, France; e-mail: rusinek@enim.fr

José A. Rodríguez-Martínez
University Carlos III of Madrid, Department of Continuum Mechanics and Structural Analysis, Madrid, Spain

Raphaël Pesci
ENSAM – Laboratory of Physics and Mechanics of Materials, FRE CNRS 3236, Metz cedex, France

Julien Capelle
National Engineering School of Metz (ENIM), Laboratory of Mechanics, Biomechanics, Polymers and Structures, Metz cedex, France

Prof. W.K. Nowacki, Solmech/2006

This paper is dedicated to our friend and colleague Prof. W.K. Nowacki who passed away on August 14, 2009.

Thank you for your kindness, humility, advice and our long French-Polish collaboration.

A thought to Alicja

In this investigation, thermo-viscoplastic behaviour of austenitic steel **AISI 304** has been characterised in tension under wide ranges of strain rate at room temperature. This metal possesses an elevated strain hardening rate and ductility which enhance its capability for absorbing energy under mechanical

loading. It has been observed that the rate sensitivity of the material is independent of plastic strain. Moreover, it has been noticed that beyond a certain level of loading rate the flow stress of the material sharply increases. In agreement with experimental evidences reported in the literature, this behaviour is assumed to be caused by the drag deformation mode taking place at high strain rates. Based on such considerations, the thermo-viscoplastic behaviour of the material has been macroscopically modelled by means of the extended Rusinek-Klepaczko model to viscous drag effects. Satisfactory matching has been found between the experiments and analytical predictions provided by the constitutive relation.

Key words: steel AISI 304, extended RK model, strain rate sensitivity, constitutive relation, thermal imaging

1. Introduction

Understanding dynamic behaviour of metallic alloys has gathered the efforts of many researchers during the last decades (Kumar *et al.*, 1968; Clifton *et al.*, 1984; Follansbee, 1986; Regazzoni *et al.*, 1987; Follansbee and Kocks, 1988; Zerilli and Armstrong, 1992; Huang *et al.*, 2009). Development of testing techniques which enable one to determine the deformation modes taking place in metallic materials at high strain rates has been a challenge approached by the most relevant experimentalists over the years (Mann, 1936; Clark and Wood, 1957; Klepaczko, 1994; Nemat-Nasser *et al.*, 2001; Nguyen and Nowacki, 1997). Thus, supported by those experimental investigations, important advances on constitutive modelling of metallic alloys have been carried out (Johnson and Cook, 1983; Zerilli and Armstrong, 1987; Nemat-Nasser and Li, 1998; Molinari and Ravichandran, 2005; Voyiadjis and Almasri, 2008; Durrenberger *et al.*, 2007-2008; Rusinek *et al.*, 2008). Derivation of constitutive descriptions capable of predicting the thermo-viscoplastic response of materials is of fundamental interest to analyse the loading processes. Important industrial sectors like automotive and naval industries are nowadays becoming more interested in replacing the traditionally used phenomenological hardening laws (Cowper and Symonds, 1952; Johnson and Cook, 1983) by more advanced physical-based constitutive descriptions (Zerilli and Armstrong, 1987; Nemat-Nasser and Li, 1998; Rusinek and Klepaczko, 2001). The latter provides a more accurate description of the material behaviour under wide ranges of loading conditions. Such an advantage allows optimization of materials used for building mechanical elements with elevated structural responsibility.

For example, experimental testing and theoretical modelling of the metallic alloys applied for construction of crash-box structures has focussed the efforts of many investigators. Among the materials specifically developed for such an application field, the **TRIP** (Transformation Induced Plasticity) steels have particularly attracted the interest of the scientific community (Fischer *et al.*, 2000; Delannay *et al.*, 2008; Rodríguez-Martínez *et al.*, 2010).

Thus, in this work, the mechanical behaviour of the high-alloy **TRIP** steel **AISI 304** has been investigated. The material has been characterised in tension under wide ranges of strain rate at room temperature. Its deformation modes have been determined. Based on such understanding of the material behaviour, **AISI 304** has been macroscopically modelled using the extended Rusinek-Klepaczko model to viscous drag effects (Rusinek and Rodríguez-Martínez, 2009). It has been proven that this physical-based constitutive relation provides an accurate description of the plastic response of the material for all the loading conditions considered.

2. Experimental characterisation of the tensile behaviour of steel AISI 304 at room temperature

Steel **AISI 304** is the most versatile and most widely used stainless steel. It has excellent forming and welding characteristics. Extensively used in a variety of industries, its typical applications include pipelines, heat exchanger railings, springs or threaded fasteners.

AISI 304 is an austenitic steel (*in the undeformed state, the microstructure of* **AISI 304** *is constituted by 100% of austenite*) containing large amount of alloying elements as **Cr** and **Ni** improving pitting and corrosion resistance, Table 1.

Table 1. Chemical composition of steel **AISI 304** [% weight] (De *et al.*, 2006)

C	Mn	Cr	Ni	Mo	Cu	Si	Nb
0.06	1.54	18.47	8.3	0.30	0.37	0.48	0.027

Next, the thermo-viscoplastic behaviour of this material is examined. Tensile experiments have been performed within wide ranges of strain rate, $10^{-4}\mathrm{s}^{-1} \leqslant \dot{\bar{\varepsilon}}^{p} \leqslant 10^{3}\mathrm{s}^{-1}$, at room temperature. The geometry and dimensions of the tensile specimens used in the characterisation are depicted in Fig. 1. The thickness of the samples is $t = 1\,\mathrm{mm}$.

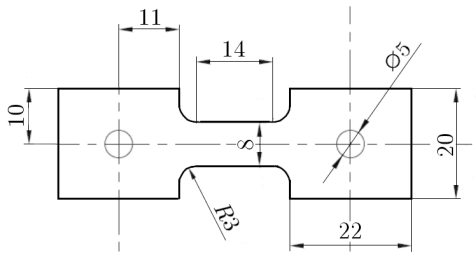

Fig. 1. Geometry and dimensions of the tensile specimens [mm] (Rusinek *et al.*, 2008)

It has to be highlighted that this specimen design allows for avoiding geometrical disturbances that frequently take place when small samples are used to reach very high strain rates during testing (Rusinek *et al.*, 2005).

2.1. Thermo-viscoplastic characterisation at low strain rates

In this section, results from the low strain rate tests performed are presented; the macroscopic behaviour of the material is illustrated in different graphs, see Figs. 2 to 3. Large ductility and an elevated strain hardening rate first characterise the mechanical behaviour of this steel, Fig. 2. Let us analyse the case of testing at $\dot{\bar{\varepsilon}}^p = 0.002\,\mathrm{s}^{-1}$; **AISI 304** reaches plasticity for $\sigma \approx 310\,\mathrm{MPa}$, from this point on the flow stress level starts to increase until the saturation condition is reached, $\sigma\Big|_{d\sigma/d\varepsilon=0} \approx 975\,\mathrm{MPa}$.

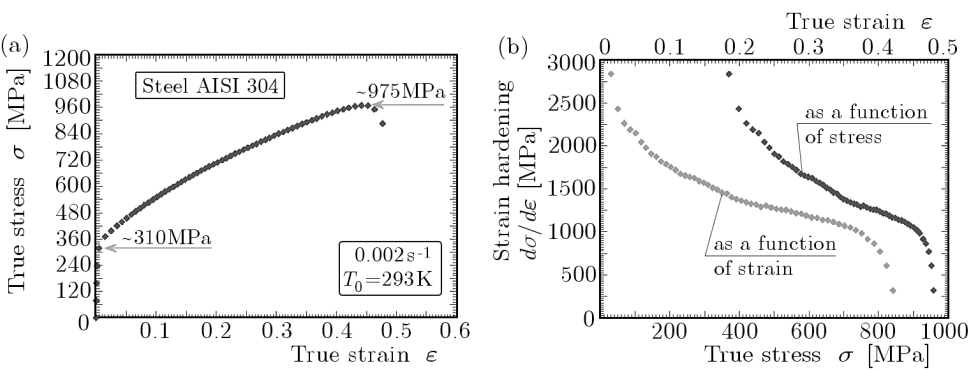

Fig. 2. (a) Flow stress evolution as a function of strain and (b) strain hardening evolution as a function of strain and stress at low strain rate and room temperature

Moreover, the low strain rate tests were filmed using a high speed infrared camera. That procedure allowed measuring the temperature increase ΔT

in the material during mechanical loading. Knowledge of the temperature increase ΔT leads to better understanding of dissipative effects taking place during material straining. These are, for example, adiabatic heating, martensitic transformation or damage mechanics as discussed in Rusinek *et al.* (2002, 2003), Nowacki *et al.* (2004).

In the following graphs, Fig. 3, the maximum increase of temperature ΔT during plastic deformation for a strain rate of $\dot{\bar{\varepsilon}}^p = 0.01\,\mathrm{s}^{-1}$ is reported. The material temperature is continuously increasing with stress and strain, Fig. 3a. It has to be noted that a non-linear relation between the temperature increase and plastic deformation is found, Fig. 3.

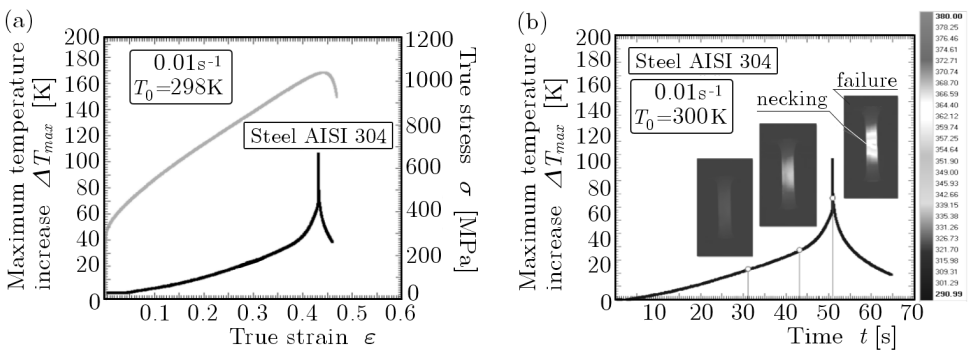

Fig. 3. (a) Maximum temperature increase and flow stress versus strain at low strain rate; (b) maximum temperature increase versus time at low strain rate

It is detected that this non-linearity is coming from two different sources:

- Dependence of the inelastic heat fraction β with plastic strain
- Dissipative effects of the martensitic transformation which takes place in this material during straining at low strain rates (Rusinek and Klepaczko, 2009).

The maximum temperature recorded during the test is close to $\Delta T_{max} \approx 110\,\mathrm{K}$, Fig. 3b. The drastic increase of temperature taking place close to the saturation stress condition has to be analysed, Fig. 3b. Such a sharp augment of the temperature occurs when necking is formed. The heat generated in the instability is hardly spread to the rest of the sample. The strong elevation of the strain rate level in the necking zone leads to local adiabatic conditions of deformation.

Next, the results obtained from the high strain rate tests are shown in order to offer a comprehensive analysis of the material rate sensitivity.

2.2. Thermo-viscoplastic characterisation at high strain rates

Flow stress evolution versus plastic strain for high loading rates is depicted in Fig. 4. Under such loading conditions the material keeps the elevated work hardening rate enhancing its ductility.

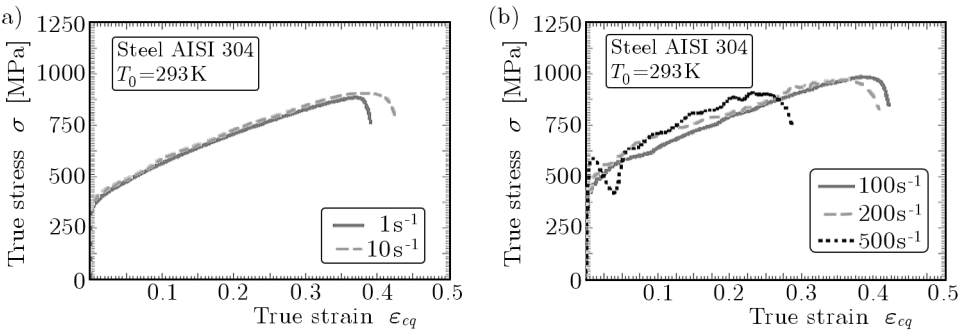

Fig. 4. Flow stress evolution as a function of strain for different high strain rate levels at room temperature

It has been noticed that the material strain hardening is kept rather constant with the loading rate variations, Fig. 4. Thus, the Volume Thermally Activated (VTA) of the material is assumed independent of the plastic strain (Taylor, 1992), Eq. (2.1)

$$V^* \approx kT \frac{\partial \ln(\dot{\overline{\varepsilon}}^p)}{\partial \overline{\sigma}^*}\bigg|_{T,\overline{\varepsilon}^p} \tag{2.1}$$

In the previous expression, Eq. (2.1), k is the Boltzmann constant and T is the absolute temperature.

It has to be noticed that beyond a certain level of loading rate, $\dot{\overline{\varepsilon}}^p \geqslant 500\,\mathrm{s}^{-1}$, the flow stress of the material sharply increases, Fig. 5. Such observation is in agreement with the experimental results reported by Follansbee (1986), Fig. 5. According to several authors (Campbell and Fergusson, 1970; Nemat-Nasser *et al.*, 2001; Rusinek and Rodríguez-Martínez, 2009) let us assume this behaviour caused by drag deformation mechanisms taking place at high strain rates (Kapoor and Nemat-Nasser, 1999).

Based on the previous considerations, the macroscopic behaviour of the **AISI 304** is modelled using the extended **RK** (Rusinek-Klepaczko) model to viscous drag effects (Rusinek and Rodríguez-Martínez, 2009). This constitutive description takes into account the independence of the material rate sensitivity with the plastic strain.

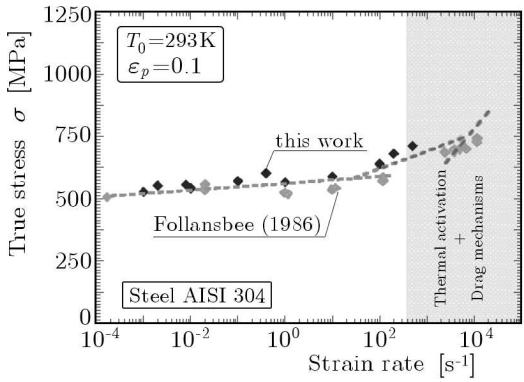

Fig. 5. Flow stress evolution as a function of the strain rate at room temperature for a strain level imposed of $\varepsilon_p = 0.1$. Comparison with the results reported by Follansbee (1986)

3. Macroscopic modelling of the thermo-viscoplastic behaviour of steel AISI 304 under wide ranges of strain rate

Next, the formulation of the extended **RK** model to viscous drag effects and the comparison of its analytical predictions with experimental results are reported.

3.1. The extended RK model to viscous drag effects

The constitutive description is based on the additive decomposition of the equivalent stress (Seeger, 1957; Zerilli and Armstrong, 1987; Nemat-Nasser and Guo, 2003; Abed and Voyiadjis, 2005; Kocks, 2001), Eq. (3.1)

$$\overline{\sigma}(\overline{\varepsilon}^p, \dot{\overline{\varepsilon}}^p, T) = \frac{E(T)}{E_0}[\sigma_\mu(\overline{\varepsilon}^p, \dot{\overline{\varepsilon}}^p, T) + \sigma^*(\dot{\overline{\varepsilon}}^p, T)] + \sigma_{vs}(\dot{\overline{\varepsilon}}^p) \tag{3.1}$$

where each term of the previous expression, Eq. (3.1), is defined below.

The multiplicative factor $E(T)/E_0$ defines Young's modulus evolution with temperature (Klepaczko, 1998), Eq. (3.2)

$$E(T) = E_0\Big\{1 - \frac{T}{T_m}\exp\Big[\theta^*\Big(1 - \frac{T_m}{T}\Big)\Big]\Big\} \qquad \forall T > 0 \tag{3.2}$$

where E_0, T_m and θ^* denote respectively Young's modulus at $T = 0\,\mathrm{K}$, the melting temperature and the characteristic homologous temperature. This expression allows for defining the material thermal softening depending on its crystal lattice (Rusinek *et al.*, 2009). In the case of **FCC** metals like the steel **AISI 304**, $\theta^* \approx 0.9$, as discussed in Rusinek *et al.* (2009).

The athermal stress reads as follows, Eq. (3.3)

$$\sigma_\mu(\overline{\varepsilon}^p, \dot{\overline{\varepsilon}}^p, T) = B(\dot{\overline{\varepsilon}}^p, T)(\varepsilon_0 + \overline{\varepsilon}^p)^{n(\dot{\overline{\varepsilon}}^p, T)} \tag{3.3}$$

It macroscopically defines dislocation interactions with long-range obstacles which determine the strain hardening rate of the material. The explicit formulas describing the modulus of plasticity $B(\dot{\overline{\varepsilon}}^p, T)$ and the strain hardening exponent $n(\dot{\overline{\varepsilon}}^p, T)$ are given by Eqs. (3.4)

$$\begin{aligned} n(\dot{\overline{\varepsilon}}^p, T) &= n_0 \Big\langle 1 - D_2 \Big(\frac{T}{T_m}\Big) \log\Big(\frac{\dot{\overline{\varepsilon}}^p}{\dot{\varepsilon}_{min}}\Big) \Big\rangle \\ B(\dot{\overline{\varepsilon}}^p, T) &= B_0 \Big\langle \Big(\frac{T}{T_m}\Big) \log\Big(\frac{\dot{\varepsilon}_{max}}{\dot{\overline{\varepsilon}}^p}\Big) \Big\rangle^{-\nu} \qquad \forall\ T > 0 \end{aligned} \tag{3.4}$$

where B_0 is the material constant, ν is proportional to temperature sensitivity, n_0 is the strain hardening exponent at $T = 0\,\mathrm{K}$, D_2 is the material constant, $\dot{\varepsilon}_{min}$ is the lower strain rate limit of the model and $\dot{\varepsilon}_{max}$ is the maximum strain rate level accepted for a particular material. The McCauley operator is defined as follows

$$\langle \bullet \rangle = \begin{cases} \bullet & \text{if} \quad \langle \bullet \rangle \geqslant 0 \\ 0 & \text{if} \quad \langle \bullet \rangle < 0 \end{cases}$$

In the following graphs, the evolution of both the modulus of plasticity $B(\dot{\overline{\varepsilon}}^p, T)$ and the strain hardening coeficient $n(\dot{\overline{\varepsilon}}^p, T)$ with temperature and strain rate, Fig. 6 is depicted. It can be observed that increasing temperature leads to diminution of the material flow stress level and strain hardening rate. It allows a proper definition of the characteristic thermal softening taking place in metallic materials subjected to high loading rates.

The thermal stress is the flow stress component defining macroscopically the rate dependent interactions with short range obstacles for the dislocation motion. It denotes the rate controlling the deformation mechanism from thermal activation. Based on the theory of thermodynamics and kinetics of slip (Kocks *et al.*, 1975), Rusinek and Klepaczko derived the following expression (Rusinek and Klepaczko, 2001), Eq. (3.5)

$$\sigma^*(\dot{\overline{\varepsilon}}^p, T) = \sigma_0^* \Big\langle 1 - D_1 \Big(\frac{T}{T_m}\Big) \log\Big(\frac{\dot{\varepsilon}_{max}}{\dot{\overline{\varepsilon}}^p}\Big) \Big\rangle^{m^*} \tag{3.5}$$

where σ_0^* is the effective stress at $T = 0\,\mathrm{K}$, D_1 is the material constant and m^* is the constant defining the reciprocity strain rate-temperature (Klepaczko, 1987).

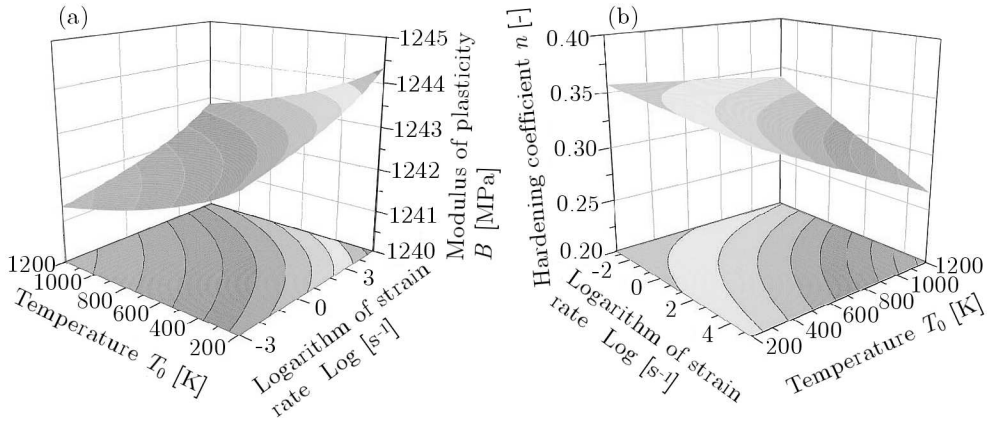

Fig. 6. Evolution of (a) modulus of plasticity and (b) strain hardening coefficient with strain rate and temperature

The formulation used for defining the viscous drag stress component is coming from the investigations due to Kapoor and Nemat-Nasser (1999). Based on theoretical considerations and supported by experimental evidences for a certain number of metals, they proposed the following relation, Eq. (3.6)

$$\overline{\sigma}_{vs}(\dot{\overline{\varepsilon}}^p) = \chi[1 - \exp(-\alpha\dot{\overline{\varepsilon}}^p)] \tag{3.6}$$

where χ is a material constant and α represents an effective damping coefficient affecting the dislocation motion (Nemat-Nasser *et al.*, 2001).

In the following graphs, the evolution of the viscous drag stress term within wide ranges of strain rate as a function of the material constants χ and α, Fig. 7 is depicted. For a strain rate $\dot{\overline{\varepsilon}}^p \leqslant 100\,\mathrm{s}^{-1}$, the viscous drag component is negligible no matter the value of previous material parameters. Moreover, it can be observed that this formulation enables one to define the two stages of the drag regime experimentally observed (Kapoor and Nemat-Nasser, 2000); the first stage of flow stress linearly increasing with the strain rate and the subsequent stage of the rate sensitivity no longer active.

In the case of adiabatic conditions of deformation, the constitutive relation is combined with the energy balance principle, Eq. (3.7). Such a relation allows for approximation of the thermal softening of the material by means of the adiabatic heating

$$\Delta T(\overline{\varepsilon}^p, \overline{\sigma}) = \frac{\beta}{\rho C_p} \int_0^{\overline{\varepsilon}^p_{max}} \overline{\sigma}(\overline{\varepsilon}^p, \dot{\overline{\varepsilon}}^p, T)\, d\overline{\varepsilon}^p \tag{3.7}$$

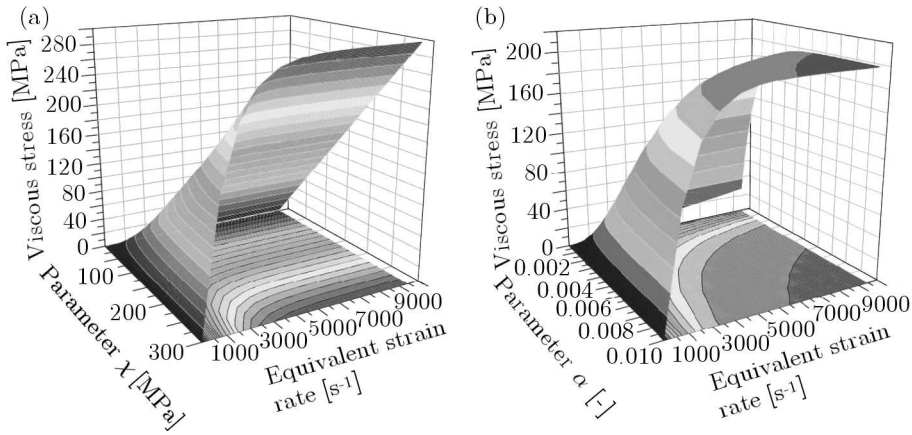

Fig. 7. Evolution of the viscous drag stress component as a function of strain rate (a) as a function of χ and (b) as a function of α

where β is the Taylor-Quinney coefficient assumed as constant, ρ is the material density and C_p is the specific heat at constant pressure. Transition from isothermal to adiabatic conditions of deformation is assumed at $\dot{\bar{\varepsilon}}^p = 10\,\mathrm{s}^{-1}$ in agreement with experimental observations reported for example in Oussouaddi and Klepaczko (1991), Berbenni *et al.* (2004).

Next, the extended **RK** model to viscous drag effects is applied to describe the thermo-viscoplastic behaviour of steel **AISI 304**.

3.2. Application of the extended Rusinek-Klepaczko model to viscous drag effects for description of the thermo-viscoplastic behaviour of steel AISI 304

Following the procedure reported by Rusinek and Rodríguez-Martínez (2009), the following material constants for calibration of the extended **RK** model are obtained, see Table 2.

Table 2. Material constants for calibration of the extended **RK** model to viscous drag effects for steel **AISI 304** Eqs. (3-1)-(3.7)

B_0 [MPa]	ν [–]	n_0 [–]	D_2 [–]	ε_0 [–]	σ_0^* [MPa]	m^* [–]
1243.6	0.001	0.36	0.035	0.0118	117.72	1.29
D_1 [–]	χ [MPa]	α [–]	θ^* [–]	$\dot{\varepsilon}_{min}$ [s^{-1}]	$\dot{\varepsilon}_{max}$ [s^{-1}]	T_m [K]
0.55	200.83	0.0009774	0.9	10^{-5}	10^{7}	1800

Conventional physical constants of the steel can be obtained from material handbooks, Table 3.

Table 3. Physical constants for steel

E_0 [GPa]	C_p [JkgK^{-1}]	β [–]	ρ [kgm^{-3}]
200	470	0.9	7800

In Fig. 8, the comparison between the experiments and analytical predictions of the model within wide ranges of strain rate $10^{-3}\,\mathrm{s}^{-1} \leqslant \dot{\bar{\varepsilon}}^{p} \leqslant 500\,\mathrm{s}^{-1}$ is illustrated. It has to be highlighted that the constitutive description enables accurate determination of the material flow stress and strain hardening for all the loading rates considered, Fig. 8.

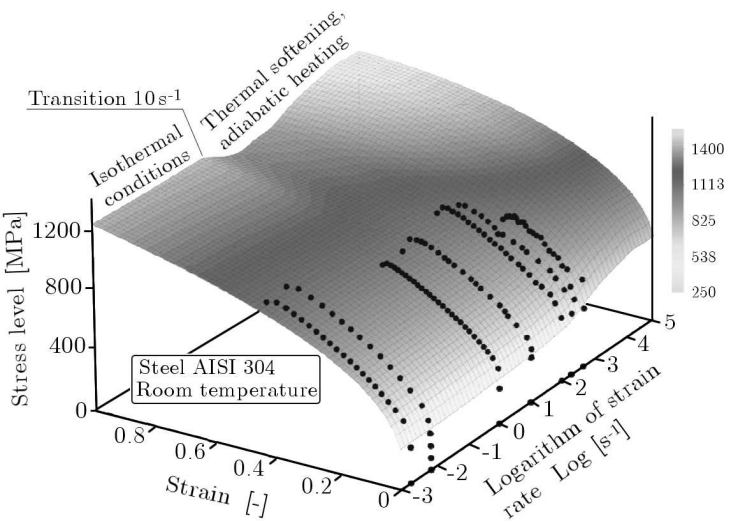

Fig. 8. Comparison between experiments and analytical predictions of the constitutive description within wide ranges of strain rate

Thus, in this investigation a predictive tool which allows proper description of the thermo-viscoplastic behaviour of steel **AISI 304** within wide ranges of loading conditions has been developed. It has to be highlighted that the constitutive description defines accurately the strain hardening and thermal softening effects observed in this material at high strain rates and large deformation.

4. Conclusions

In this work, the thermo-viscoplastic behaviour of steel **AISI 304** has been characterised in tension under wide ranges of strain rates at room temperature. The material shows high strain hardening and ductility for the whole range of loading conditions tested. It has been found that the rate sensitivity of the material is independent of plastic strain. Moreover, based on the experiments reported by Follansbee (1986), it has been observed that **AISI 304** shows viscous drag effects at high strain rates. Thus, the material response under loading has been modelled using the extended **RK** model to viscous drag effects. It provides an accurate description of the material behaviour for all the loading conditions analysed. Thus, in this investigation a predictive tool for a proper definition of the thermo-mechanical response of steel **AISI 304** within wide ranges of strain rates has been developed.

Acknowledgements

The authors express their thanks to Mr. Philippe and Mr. Tobisch from the company **Zwick** for the facilities conferred to perform the tests at high strain rates.

References

1. Abed F.H., Voyiadjis G.Z., 2005, Plastic deformation modeling of AL-6XN stainless steel at low and high strain rates and temperatures using a combination of BCC and FCC mechanisms of metals, *Int. J. Plasticity*, **21**, 1618-1639
2. Berbenni S., Favier V., Lemoine X., Berveiller N., 2004, Micromechanical modelling of the elastic-viscoplastic behaviour of polycrystalline steels having different microstructures, *Mater. Sci. Eng.*, **372**, 128-136
3. Campbell J.D., Ferguson W.G., 1970, The temperature and strain-rate dependence of the shear strength of mild steel, *Philos. Mag.*, **81**, 63-82
4. Clark D.S., Wood D.S., 1957, The influence of specimen dimension and shape on the results in tension impact testing, *T. Am. Soc. Mech. Eng.*, **5**, 77-85
5. Clifton R.J., Duffy J., Hartley K.A., Shawki T.G., 1984, On the critical conditions for shear band formation at high strain rates, *Scripta Metall.*, **5**, 443-448
6. Cowper G.R., Symonds P.S., 1952, Strain hardening and strain rate effects in the impact loading of cantilever beams, Brown Univ., Div. of Appl. Mech., Report no. 28

7. De A.K., Speer J.G, Matlock D.K., Murdock D.C., Mataya M.C., Comstock R.J., 2006, Deformation-induced phase transformation and strain hardening in type 304 austenitic stainless steel, *Metall. and Mat. Trans.*, **A 37**, 1875-1886

8. Delannay L., Jacques P., Pardoen T., 2008, Modelling of the plastic flow of trip-aided multiphase steel based on an incremental mean-field approach, *Int. J. Solids. and Struct.*, **45**, 1825-1843

9. Durrenberger L., Klepaczko J.R., Rusinek A., 2007, Constitutive modeling of metals based on the evolution of the strain-hardening rate, *Journal of Engineering Materials and Technology*, **129**, 550-558

10. Durrenberger L., Molinari A., Rusinek A., 2008, Internal variable modeling of the high strain-rate behavior of metals with applications to multiphase steels, *Materials Science and Engineering*, **A 478**, 297-304

11. Fischer F.D., Reisner G., Werner E., Tanaka K., Cailletaud G., Antretter T., 2000, A new view on transformation induced plasticity (TRIP), *Int. J. Plasticity*, **16**, 723-748

12. Follansbee P.S., 1986, High-strain-rate deformation of FCC metals and alloys, *Metallurgical Applications of Shock-Wave and High-Strain-Rate Phenomena*, 451-479

13. Follansbee P.S., Kocks U.F., 1988, A constitutive description of the deformation of copper based on the use of the mechanical threshold stress as an internal state variable, *Acta Metall.*, **1**, 81-93

14. Huang M., Rivera-Díaz-del-Castillo P.E.J., Bouaziz O., Van der Zwaag S., 2009, A constitutive model for high strain rate deformation in FCC metals based on irreversible thermodynamics, *Mech. Mat.*, **41**, 982-988

15. Johnson G.R., Cook W.H., 1983, A constitutive model and data for metals subjected to large strains, high strain rates and high temperatures, In: *Proceedings of Seventh International Symposium on Ballistics*, 541-547

16. Kapoor R., Nemat-Nasser S., 1999, Comparison between high strain-rate and low strain-rate deformation of tantalum, *Metall. Mater. Trans.*, **A 31**, 815-823

17. Klepaczko J.R., 1987a, A general approach to rate sensitivity and constitutive modeling of FCC and BCC metals, In: *Impact: Effects of Fast Transient Loadings*, Rotterdam, 3-35

18. Klepaczko J.R., 1987b, A practical stress-strain-strain rate-temperature constitutive relation of the power form, *J. Mech. Work Technol.*, **15**, 143-165

19. Klepaczko J.R., 1994, An experimental technique for shear testing at high and very high strain rates. The case of a mild steel, *Int. J. Impact Eng.*, **15**, 25-39

20. Kocks U.F., 2001, Realistic constitutive relations for metal plasticity, *Mat. Sci. and Eng.*, **A 317**, 181-187

21. Kocks U.F., Argon A.S., Ashby M.F., 1975, Thermodynamics and kinetics of slip, In: Chalmers B., Christian J.W., Massalski T.B. (Eds.), *Progress in Materials Science*, **19**, Pergamon Press, Oxford

22. Kumar A., Hauser F.E., Dorn J.E., 1968, Viscous drag on dislocations in aluminum at high strain rates, *Acta Metall.*, **9**, 1189-1197

23. Mann H.C., 1936, High-velocity tension-impact tests, *Proc. ASTM*, **36**, 85

24. Molinari A., Ravichandran G., 2005, Constitutive modeling of high-strain-rate deformation in metals based on the evolution of an effective microstructural length, *Mech. Mat.*, **37**, 737-752

25. Nemat-Nasser S., Guo W.G., 2003, Thermomechanical response of DH-36 structural steel over a wide range of strain rates and temperatures, *Mech. Mat.*, **35**, 1023-1047

26. Nemat-Nasser S., Guo W.G., Kihl D.P., 2001, Thermomechanical response of AL-6XN stainless steel over a wide range of strain rates and temperatures, *J. Mech. Phys. Solids*, **49**, 1823-1846

27. Nemat-Nasser S., Li Y., 1998, Flow stress of FCC polycrystals with application to OFHC Copper, *Acta Mater.*, **46**, 565-577

28. Nguyen H.V., Nowacki W.K., 1997, Simple shear of metal sheets at high rates of strain, *Arch. of Mech.*, **49**, 369-384

29. Nowacki W.K., Rusinek A., Gadaj S.P., Klepaczko J.R., 2004, Temperature and strain rate effects on TRIP sheet steel. Measurement of temperature by infrared thermograph, *Proceeding 21th international congress of Theoretical and Applied Mechanics, ICTAM 2004*

30. Oussouaddi O., Klepaczko J.R., 1991, An analysis of transition from isothermal to adiabatic deformation in the case of a tube under torsion, *Proceedings Conf. DYMAT 91, Journal de Physique IV*, Coll. C3 (Suppl. III), C3-323 [in French]

31. Regazzoni G., Kocks U.F., Follansbee P.S., 1987, Dislocation kinetics at high strain rates, *Acta Metall.*, **12**, 2865-2875

32. Rodríguez-Martínez J.A., Pesci R., Rusinek A., Arias A., Zaera R., Pedroche D.A., 2010, Thermo-mechanical behaviour of TRIP 1000 steel sheets subjected to low velocity perforation by conical projectiles at different temperatures, *Int. J. Solids and Structures*, **47**, 1268-1284

33. Rusinek A., Cheriguene R., Baumer A., Larour P., 2008, Dynamic behavior of high-strength sheet steel in dynamic tension: experimental and numerical analyses, *J. of Strain Analysis for Engineering*, **43**, 37-53

34. Rusinek A., Gadaj S.P., Nowacki W.K., Klepaczko J.R., 2002, Heat exchange simulation during quasi-static simple shear of sheet steel, *J. Theoretical Appl. Mech.*, **40**, 317-337

35. Rusinek A., Klepaczko J.R., 2001, Shear testing of sheet steel at wide range of strain rates and a constitutive relation with strain-rate and temperature dependence of the flow stress, *Int. J. Plasticity*, **17**, 87-115

36. Rusinek A., Klepaczko J.R., 2009, Experiments on heat generated during plastic deformation and stored energy for TRIP steels, *Mater. Design*, **30**, 35-48

37. Rusinek A., Nowacki W.K., Gadaj S.P., Klepaczko J.R., 2003, Measurement of temperature coupling by thermovision and constitutive relation at high strain rates for dual phase sheet steel, **J. Phys. IV**, **110**, 411-416

38. Rusinek A., Rodríguez-Martínez J.A., 2009, Thermo-viscoplastic constitutive relation for aluminium alloys, modeling of negative strain rate sensitivity and viscous drag effects, *Mater. Des.*, **30**, 4377-4390

39. Rusinek A., Rodríguez-Martínez J.A., Klepaczko J.R., Pecherski R.B., 2009, Analysis of thermo-visco-plastic behaviour of six high strength steels, *Mater. Design*, **30**, 1748-1761

40. Rusinek A., Zaera R., Klepaczko J.R., Cheriguene R., 2005, Analysis of inertia and scale effects on dynamic neck formation during tension of sheet steel, *Acta Mat.*, **53**, 5387-5400

41. Seeger A., 1957, The mechanism of glide and work-hardening in face centered cubic and hexagonal close-packed metal, In: *Dislocations and Mechanical Properties of Crystals*, J. Wiley, New York

42. Taylor G., 1992, Thermally-activated deformation of BCC metals and alloys, *Prog. Mater. Sci.*, **36**, 29-61

43. Voyiadjis G.Z., Almasri A.H., 2008, A physically based constitutive model for FCC metals with applications to dynamic hardness, *Mech. Mat.*, **40**, 549-563

44. Zerilli F.J., Armstrong R.W., 1987, Dislocation-mechanics-based constitutive relations for material dynamics calculations, *J. Appl. Phys.*, **61**, 1816-1825

45. Zerilli F.J., Armstrong R.W., 1992, The effect of dislocation drag on the stress-strain behaviour of FCC metals, *Acta Metall. Mater.*, **40**, 1803-1808

Modelowanie i doświadczalna weryfikacja termo-lepkosprężystych właściwości stali AISI 304 w szerokim zakresie prędkości odkształceń w temperaturze pokojowej

Streszczenie

W pracy scharakteryzowano termo-lepkosprężyste właściwości stali AISI 304 na podstawie prób rozciągania dla szerokiego zakresu prędkości odkształceń w temperaturze pokojowej. Stal ta posiada podwyższoną ciągliwość i stopień umocnienia odkształceniowego, które to cechy powiększają jej zdolność do pochłaniania energii mechanicznej. Zaobserwowano, że wrażliwość stali na tempo obciążeń jest niezależna od wartości odkształceń plastycznych. Co więcej, zauważono, że powyżej pewnej prędkości zmian obciążenia naprężenie płynięcia materiału gwałtownie rośnie. W zgodzie z rezultatami badań doświadczalnych opisanymi w literaturze założono, że zachowanie takie wywołane jest pojawieniem się tłumionej postaci deformacji charakterystycznej dla wysokich prędkości odkształcenia. Na podstawie przeprowadzonych badań zaproponowano makroskopowy model termo-lepkosprężystych właściwości stali w oparciu o rozszerzony model Rusinka-Klepaczki dla odzwierciedlenia efektu oporu wiskotycznego. Otrzymano zadawalającą korelację pomiędzy wynikami uzyskanymi z konstytutywnego modelu materiału oraz rezultatami badań doświadczalnych.